SAFETY MANAGEMENT SYSTEM ARCHITECTURE OF UAV IN URBAN AREA

1. INTRODUCTION

Due to rapidly changing system designs, lack of quality assurance procedures, and the use of non-standardized components, the unmanned aerial vehicle (UAV) carry a considerable amount of uncertainty when it comes to establishing airworthiness assessments and regulatory procedures.

1.1 BACKGROUND & MOTIVATION

Singapore imposed a UAV regulation through Civil Aviation Authority of Singapore (CAAS) with launching online portal for drone operators permit application and activity permit is required for flying drones that weigh more than 7 kg for any purpose, business, or recreation (Kok, 2015). Those who fly drones for business purposes are required to apply for both permits regardless of the weight of the aircraft. Recreation or research drones do not require a permit if the weight of the aircraft is less than 7 kg (CAAS, 2019).

For the operation rule, CAAS also published regulations that describe the operating requirements for both Visual Line of Sight (VLOS) and Beyond Visual Line of Sight (BVLOS) that with certain restrictions and pilot ratings, exceptions to the constant VLOS requirement are possible.

However, many commercial use cases necessitate BVLOS operations over the general population to achieve full benefits (e.g., infrastructure inspection or parcel delivery). The mechanism that causes harm on human and ground properties is then has been set as base of the safety level in this study, where the harm occurs when an UAV falls from a given height at a given kinetic energy level onto a person/ground facility below. Other forms of harm on UAV itself are not be considered in this study.

1.2 GENERAL SYSTEM PROTOTYPE & CONCEPT OF OPERATION

There are variations among different types of unmanned aircraft vehicles and for the purpose of this study, the core sets of functions that most of unmanned aircraft vehicles will need in routinely and safely operations within Singapore National Airspace System are identified.

2. SAFETY MANAGEMENT MODEL

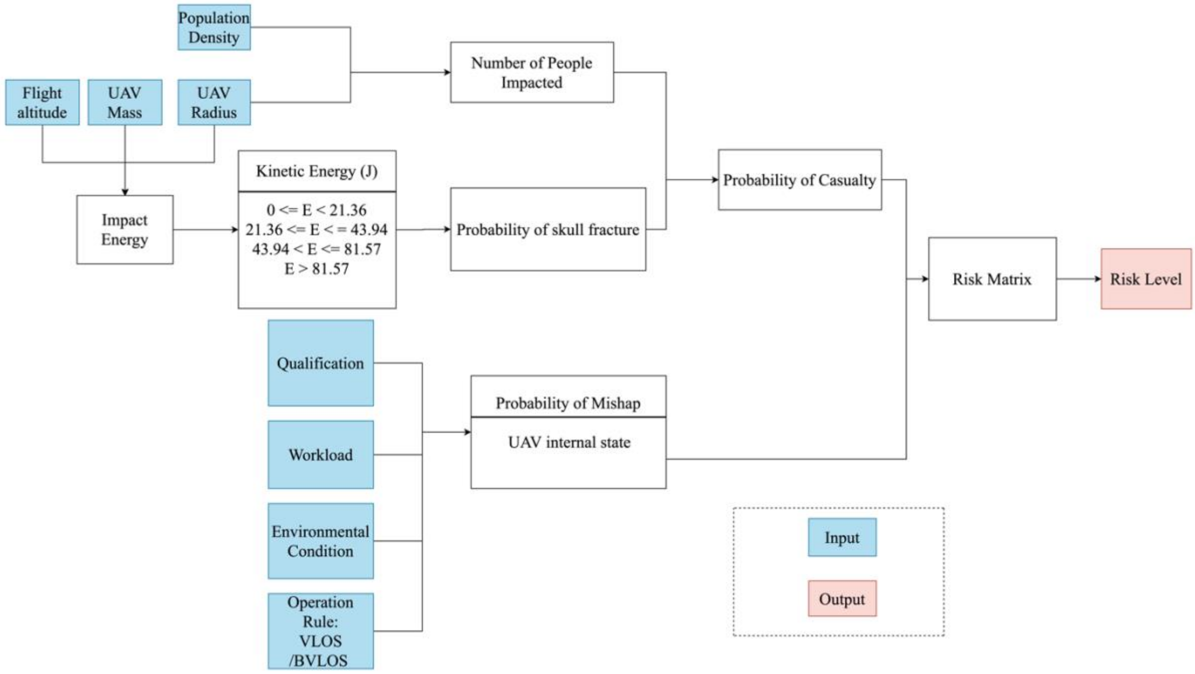

This study aims to provide a model for assessing the risk level before each UAV using the probability of casualty, the probability of mishap in a risk matrix.

The research begin with an overview of database for obtaining basic data sense on previous UAV accidents/incidents over the past decades, followed by a categorization of the types of mishaps for creating the Bayesian Network model to calculate the probability of a UAV mishap.

Section 4 provides an analysis of the relationship among the kinetic energy of UAV falling from a certain range of altitude, the impact force of a UAV free fall and the probability of skull fracture, followed by the probability of a specific person being exposed to a UAV mishap (free fall) using basic math.

The study concludes the risk level result with the risk matrix.

3. PROBABILITY OF MISHAP

3.1 HISTORICAL DATA REVIEW

One of the challenges associated with UAV risk management is the limited amount of historical/operational data which prohibits adequate UAV component and system reliability estimations (Ancel, Capristan, Foster, & Condotta, 2019).
In order to investigate current UAV accidents/incidents, Aviation Safety Reporting System (ASRS) database was considered for review and categorization and all accidents/incidents between 2000 and 2020 involving unmanned aerial aircraft were selected.
A total of 170 accidents/incidents for years 2000-2020 constitute the initial UAV accidents for this study and it is likely that current listed database are not a complete record and a greater number and variety of accidents/incidents can be expected in the future.

3.1.1 GENERALIZED ACCIDENT TYPES

This research categorized the 170 UAV accident/incident cases by their primary problem as below table:

Primary Problem	Number of Cases
Human Factors	85
Procedure	34
Aircraft	20
Ambiguous	17
Weather	4
Company Policy	3
Airspace Structure	2
Chart or Publication	2
ATC	1
Equipment Tooling	1
-	1

Given the information from above table, these cases were reviewed from three main aspects and all the cases contain either a single or combination of them; namely, internal state of aircraft system (UAV), human factors (HF) and external environment (EE). The cases were grouped into seven main categories in terms of three main perspectives and the frequency of their occurrences is given in below figure.

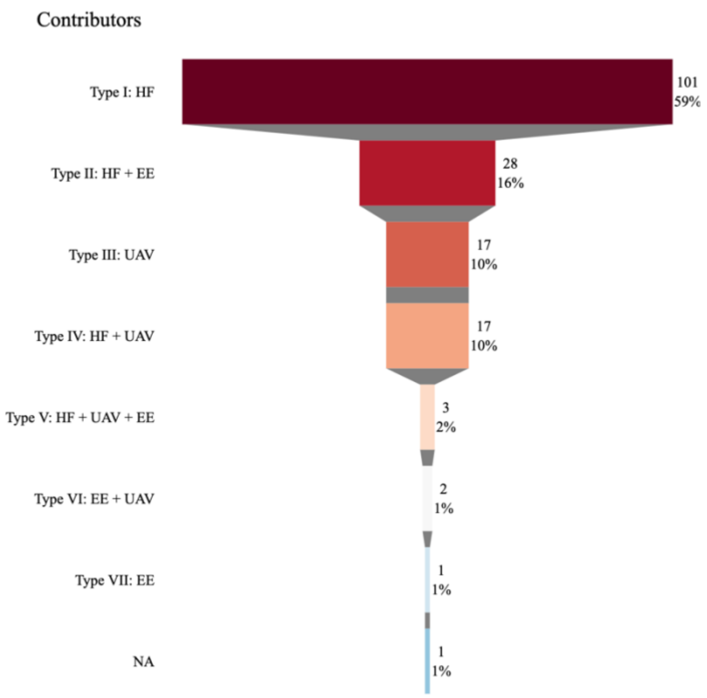

Out of the 170 cases, only 17 cases are directly related to a UAV system or component issue (Type III – UAV, 10%) and only 1 case is directly related to external environment (Type VII – EE, 1%). The remaining 151 cases (89%) all include human error, directly or indirectly. Human error including UAV operator error, procedure and chart/publication error and impropriate company policy was observed in 101 cases (Type I – 59%). In 28 of the cases were related to a combination of adverse environmental condition coupled with human errors (Type II – 16%) while 17 cases were found to be a combination of UAV system or component failure coupled with human errors (Type IV – 10%). Three cases were observed to be involved with all three primary problems (Type V – 2%).

Although not shown, this research conducted an extensive semantics analysis of ASRS narrative reports on selected 170 cases and it is indicated that 60% of Type I, II, IV and V accidents were related to human operator lack of situational awareness. Such awareness, is defined as “a prerequisite to rational decision making and reflects a humans ability to perceive elements in their environment, comprehend their meaning and project their state into the future" (Dzindolet, Pierce, Beck, Dawe, & Anderson, 2001). Apart from the awareness of elements in the environment, the term of "situation" in this context also includes human-UAV interaction that the loss of situational awareness happens as UAV operator's mental model starts to deviate from reality, such as being distracted (Nguyen, Lim, Nguyen, Gordon-Brown, & Nahavandi, 2019).

3.2 PROBABILISTIC GRAPHICAL MODEL

The Bayesian method was found to be suitable to represent complex aviation safety accidents where multi-dependent causal factors are prominent (Ancel et al., 2015). A Bayesian Network (BN) classifier, which results in a directed acyclic graph with a set of nodes that denotes the variables, is a learning probabilistic model that useful for diagnosis, prediction, classification and decision-making from the obtained data, was selected in this study for reasoning under uncertainty.

Based on the classification of accidents/incidents given above, a generic framework for the Bayesian probabilistic graphical model is given in below figure for visualizing the model concept and identifying the interaction among internal state of aircraft system, human factors and the external environment.

The BN modelling in this study is implemented as a probabilistic graphical modelling method to estimate UAV mishap likelihood and the data for conditional probability tables behind each node is inferenced based on fusing the ASRS database, Nonelectronic Parts Reliability Data Publication (NPRD-2016) database, the estimation from (Abdallah, 2019) and the subject matter expert opinions. Through model construction, Bayesian networks can be used as efficient tools for knowledge discovery and data mining (Heckerman, 2008).

According to conditional dependency of variables and chain rules, the joint probability distribution of a set of variables in BN is given by (Jensen & Nielsen, 2001):

$$P(S) = \prod_{i=1}^{n-1} P\ (X_i | X_{i+1}, \dots, X_n)$$

Where $S = \{X_1, X_2, \dots, X_n\}$ and X_{i+1} is the parent of X_i.

Further, based on Bayes theorem the updated prior probability of an event I is given by:

$$P\ (S|I) = \frac{P(S \cap I)}{P(I)}$$

Where in the case of this study $S = \{U, H, E\}$ that U is the internal state of UAV system, H is the human factor while E is the environmental condition as detailed discuss in later section.

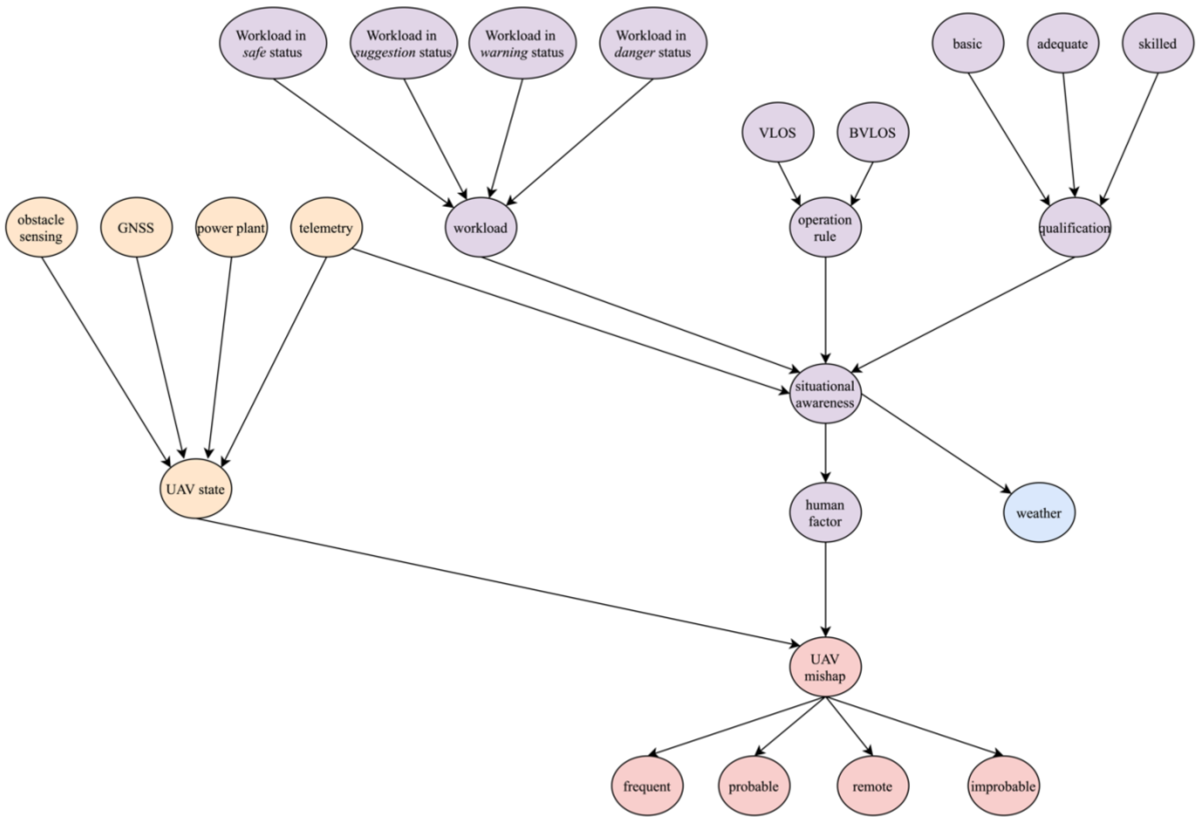

3.2.1 HUMAN FACTOR

As discussed in above section, human operator lack of situational awareness is one of the main causes of UAV mishaps. This study recognizes human factor as UAV operator interacts with environmental conditions and UAV system states through his/her subjective perception and knowledge. The human factor can be expressed as:

$$H = SA \cup RL$$

Where SA is the situational elements that define the environmental and vehicle situation including weather, ground obstacles, Notice to Airman, relevant UAV regulations and rules, airspace restriction, other aircraft, UAV internal state, etc.

Human operator's perception of situational elements SA in this study is defined as:

$$SA = \{WL, QL, RL\}$$

Where WL is the workload of human operator, QL is the qualification factor of human operator and RL is the operating rule as shown on below directed acyclic subnetwork graph .

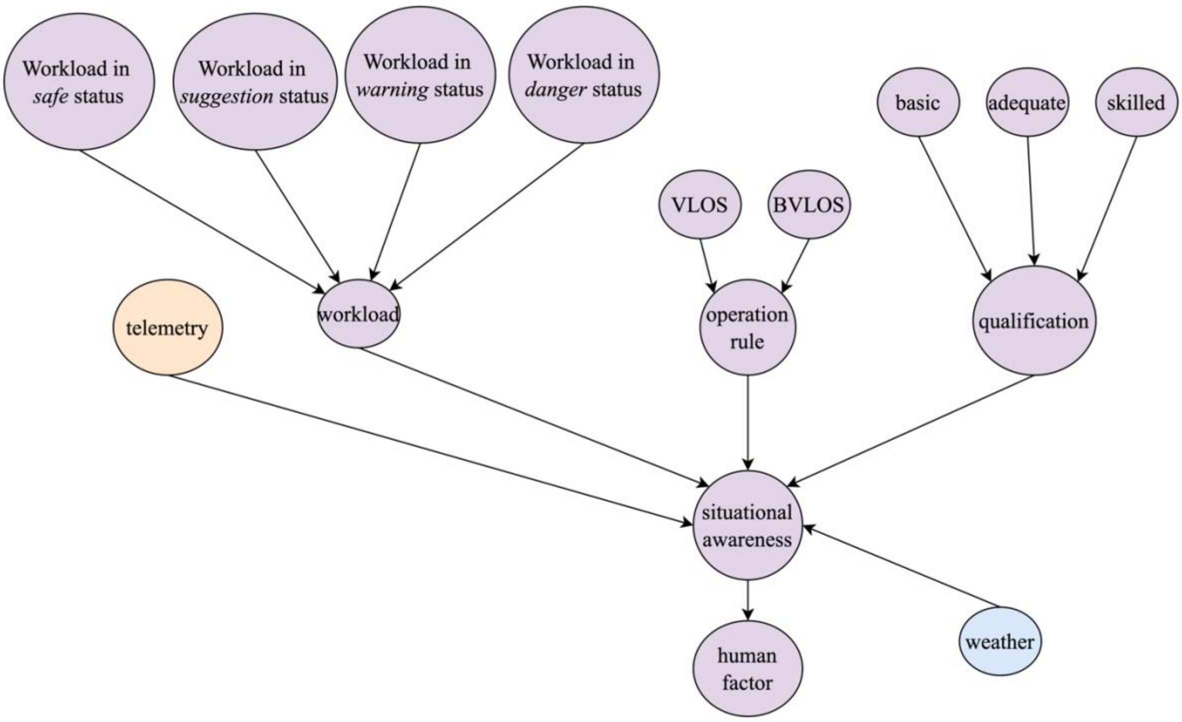

3.2.2 WORKLOAD MODULE

Subjective workload assessment techniques are popular due to their ease of use and sensitivity to workload variations (Reid & Nygren, 1988).

The workload assessing dimension in this study adapts the work done by NASA-TLX (Task Load Index) (Hart & Staveland, 1988) for multidimensional cognitive evaluation to represent the probability of UAV operators being fatigue in achieving a specific level of performance. Before a flight, the human operator will be asked to fill NASA-TLX questionnaire for evaluating his/her subjective workload on a five-dimensions scale regarding: mental demand, physical demand, temporal demand, overall performance and effort, with a weighted score from 0 to 100.

The resulting workload module is calculated as following table that when the final overall score is between 0 to 25, the workload is assumed in *safe* status. When the final overall score is between 26 to 50, the workload is assumed in *suggestion* status. When the final overall score is between 51 to 70, the workload is assumed in *warning* status. When the final overall score is between 71 to 100, the workload is assumed in *danger* status.

The conditional probabilities for fatigue based on workload is shown as below figure.

Dimension	Weighting scores	Rating Score (0-100 for each dimension) Description
Mental Demands	0.3	How much mental and perceptual activity do you think it will be required in this flight (e.g.: thinking, deciding, calculating, remembering, looking, etc.)?
Physical Demands	0.2	How much physical activity do you think it will be required in this flight (e.g.: pushing, pulling, turning, controlling, communicating, navigating, etc.)?
Temporal Demands	0.3	How much time pressure do you think it will be due to the pace during the flight?
Overall Performance	0.1	How confidence do you think you will be in performing this flight?
Effort	0.1	How hard do you think you will have to work (mentally and physically) to accomplish your level of performance?

Pre-flight self-rating table for measuring operator's workload

Score	Description
0-25	Workload in *safe* status
26-50	Workload in *suggestion* status
51-75	Workload in *warning* status
76-100	Workload in *danger* status

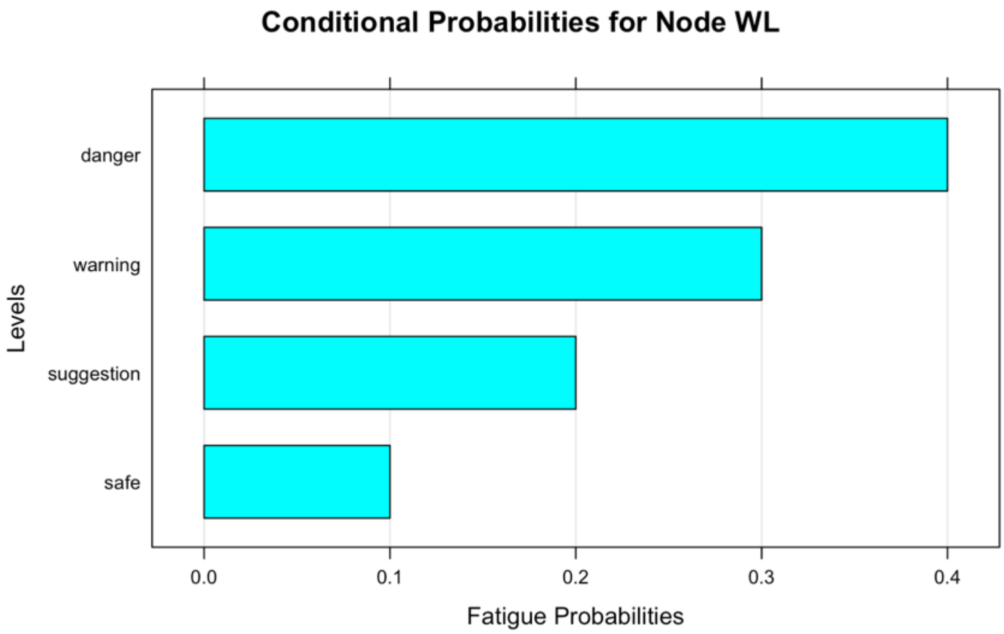

3.2.3 QUALIFICATION MODULE

The minimum training requirements for UAV pilots under CAAS rules is 2 hours for relevant theoretical knowledge. The resulting qualification assessment module as following table is used to represent the probability of an operator lack knowledge of relevant UAV regulations, rules, restrictions, and the probability of misjudging the weather.

When pilot's training and experience is less than 30 hours, the qualification module is assumed to be *basic*. When pilot's training and experience is between 30 to 100 hours, the qualification module is assumed to be *adequate*. When pilot's training and experience is more than 100 hours, the qualification module is assumed to be *skilled*.

Training/Experience Hour	Description
2-30	*basic*
30-100	*adequate*
> 100	*skilled*

The conditional probabilities for operator being inexperience based on training hour is shown as below figure.

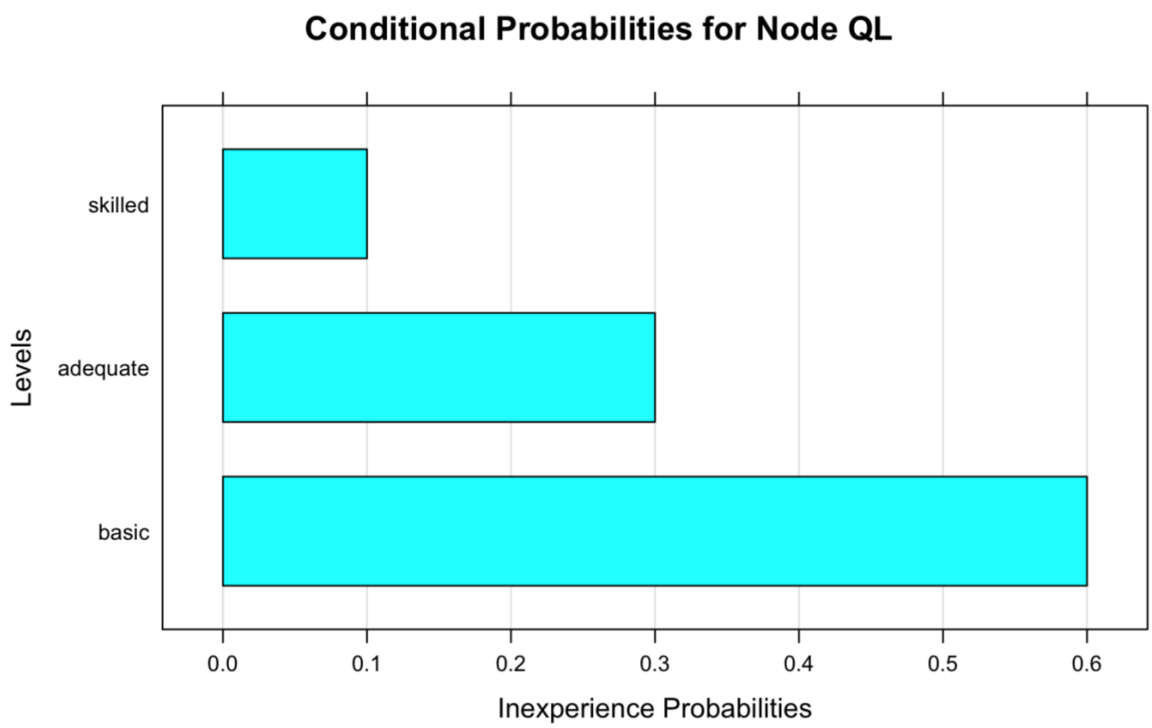

3.2.4 OPERATION RULE

The operation rule is defined as:

$$Rl = \{VS, BS\}$$

where VS and BS refers to VLOS and BVLOS respectively.

For systems operating in BVLOS environments, all information possessed by the vehicle equipped with an Automated Dependent Surveillance Broadcast is shared with the operator by telemetry link and the failure probability of situational awareness of an operator under BVLOS can be expressed as:

$$P(\overline{H}) = P\ (\overline{SA}|T, BS) + \ P\ (\overline{SA}|\overline{T}, BS)$$

Where $P(T)$ is the reliability of the telemetry.

Given the nature of VLOS, this study assumes that the human operator is able to reason about the vehicle state without additional telemetry communication and, in such operating condition the failure probability of situational awareness of an operator is given by:

$$P(\overline{H}) = P\ (\overline{SA}|VL)$$

3.3 UAV INTERNAL SYSTEM

A simplified and generalized diagram of current UAV architecture considering all possible main subsystems is shown on below figure.
It is important to recall that the aim of this UAV model is to represent vehicle weighting 7kg or below. In this context, this study only demonstrates high-level aircraft systems and not considered to be comprehensive.

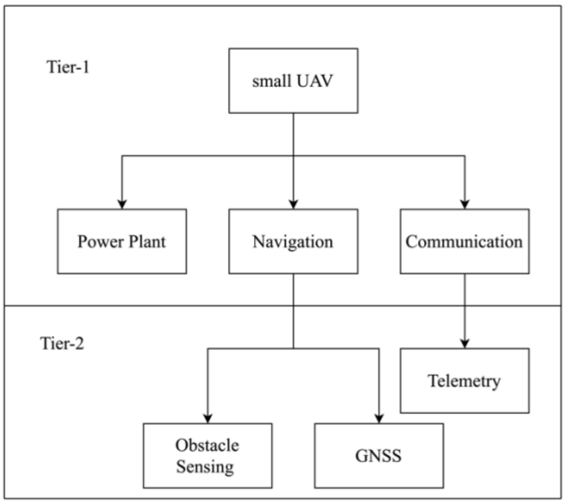

UAV system architecture is given by:

$$U = \{PO, OB, GS, FC, T\}$$

Where PO, OB, GS, FC, T refers the power plant, obstacle sensor, Global Navigation Satellite Systems, on-board flight computer and the telemetry link of the vehicle respectively as shown on figure subnetwork of the BN.

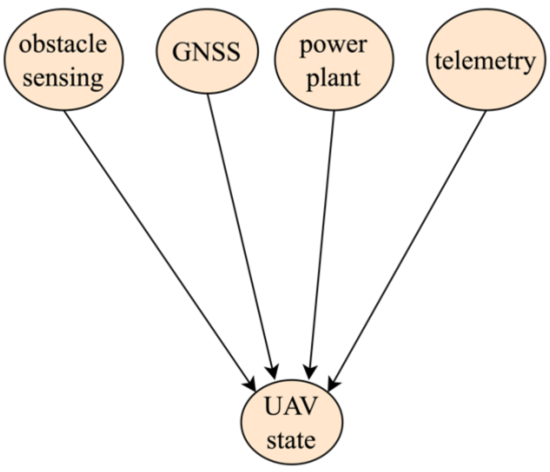

3.4 ENVIRONMENTAL CONDITION

Small UAV is easily, adversely affected by inclement weather conditions (Jensen & Nielsen, 2001). Despite regional weather hourly information and forecasts are available by local weather reports such as MEATR and TAF from weather station, it is recorded that UAV flights were occasionally aborted under both VLOS and BVLOS after experienced undesirable vehicle performance as a result of adverse weather such as turbulence, low visibility, icing, etc.

For the probability of loss of weather awareness we have:

$$P(\bar{E}) = P(\,\overline{BW} \mid \bar{H}\,)$$

Where $P(\,\overline{BW} \mid \bar{H})$ is the probability of the UAV operator misjudge bad weather information.

3.5 BAYESIAN NETWORK MODELLING

R programming package *bnlearn* is used in this study for Bayesian network creating and inference. *Bnlearn* is designed to provide a flexible simulation suite for methodological research and effective and scalable data analysis tools for working with BNs on real-world data. This is achieved by a modular architecture in which algorithms are decoupled from model assumptions, to make it possible to mix and match the methods found in the literature.

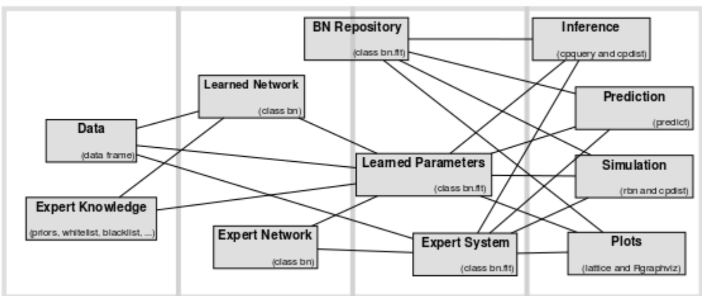

The key points include:

- *Creating the structure of the network manually, gives an object of class BN that encodes S:*

Recall that the objects of class BN and each node of them are encoded as shown on figure above, the parameters used for learning the structure is derived from historical and expert subjective domain data as stated in former section.

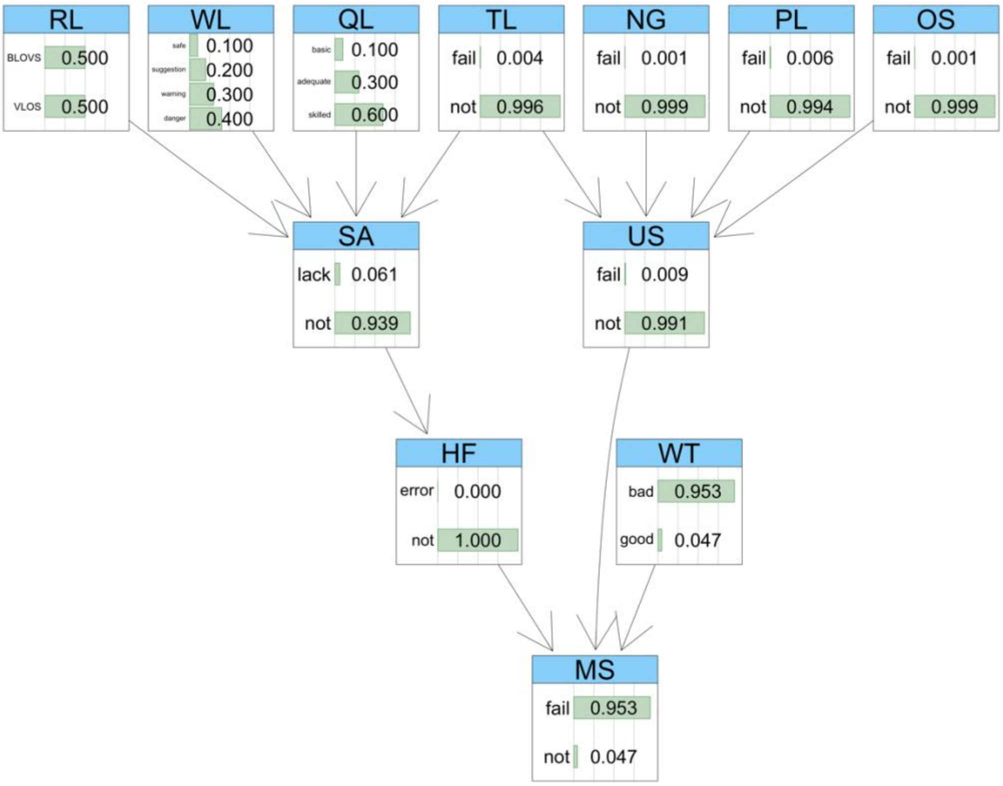

- *Learning the parameters for a given structure starts from a BN object and gives a fitted object of class BN that encodes (S, Θ):*

This study generates 10 random samples for simple illustration as shown on below table.

RL	WL	QL	SA	TL	NG	PL	OS	US	WT	HF	MS
VLOS	suggestion	skilled	not	not	not	not	not	not	bad	not	fail
VLOS	danger	adequate	not	not	not	not	not	not	good	not	not
BLOVS	suggestion	skilled	not	not	not	not	not	not	good	not	not
VLOS	danger	skilled	not	not	not	not	not	not	good	not	not
VLOS	danger	skilled	not	not	not	not	not	not	bad	not	fail
BLOVS	danger	adequate	not	not	not	not	not	not	bad	not	fail
BLOVS	danger	adequate	not	not	not	not	not	not	bad	not	fail
BLOVS	safe	skilled	not	not	not	not	not	not	bad	not	fail
BLOVS	warning	adequate	not	not	not	not	not	not	good	not	not
VLOS	warning	skilled	not	not	not	not	not	not	good	not	not

- Computing maximum a posteriori (MAP) queries:

The goal of a MAP query is to find the combination of values for (a subset of) the variables in the network that has the highest probability given some evidence. If the evidence is a partially-observed new individual, then performing a MAP query amounts to a classic prediction exercise.

Under VLOS operation rule that human operator’s workload is in *danger* status and his/her qualification is *basic* while the weather condition is *good*, the probability of UAV mishap is 0.001.

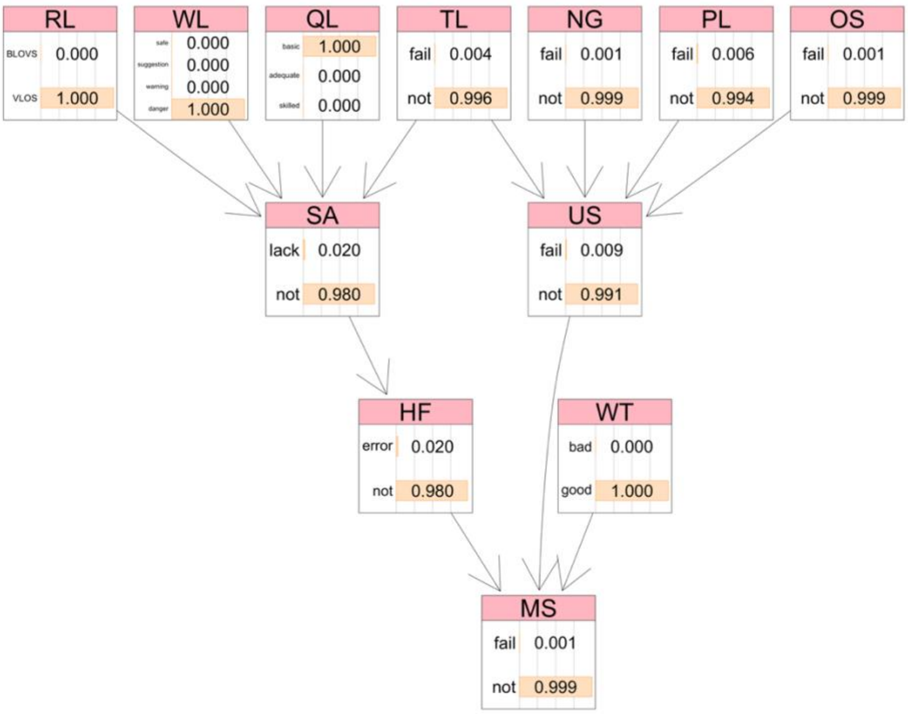

However, when the weather condition is *bad* and other conditions are the same as stated above, the probability of UAV mishap is 1.

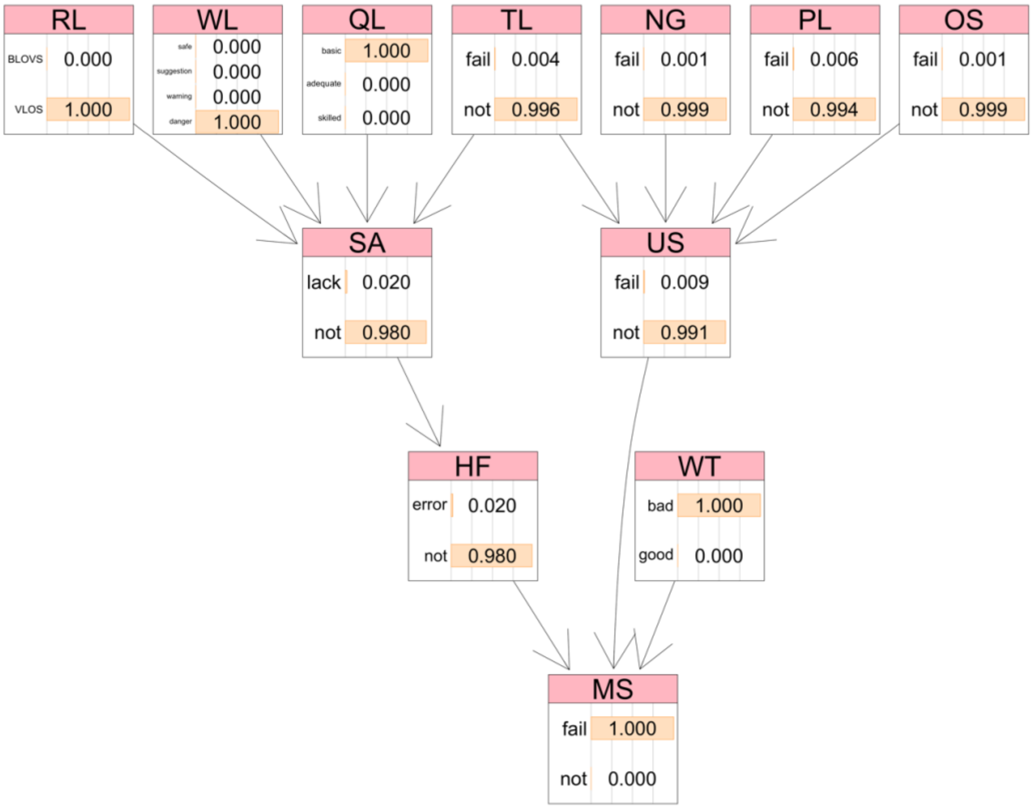

RL
BLOVS 0.000
VLOS 1.000
WL
safe 0.000
suggestion 0.000
warning 0.000
danger 1.000
QL
basic 1.000
adequate 0.000
skilled 0.000
TL
fail 0.004
not 0.996
NG
fail 0.001
not 0.999
PL
fail 0.006
not 0.994
OS
fail 0.001
not 0.999
SA
lack 0.020
not 0.980
US
fail 0.009
not 0.991
HF
error 0.020
not 0.980
WT
bad 1.000
good 0.000
MS
fail 1.000
not 0.000

4. PROBABILITY OF CASUALTY

This study adopts six popular small UAV as study models whose parameters are provided as below table:

UAV Type	Model	Mass (kg)	Diameter (m)	Radius(m)
DJI Mavic Mini	Model 1	0.249	0.245	0.1225
DJI Mavic Air 2	Model 2	0.570	0.183	0.0195
DJI Mavic 2 Pro	Model 3	0.907	0.322	0.161
DJI PHANTOM 4 PRO V2.0	Model 4	1.375	0.350	0.175
YUNTYHPRBPUS	Model 5	1.633	0.520	0.26
YUNTYH3EU	Model 6	1.985	0.520	0.26

4.1 FREE FALL IMPACT KINETIC ENERGY ESTIMATION

This section analyses when the UAV power plant fails that it is a free fall experiencing a downward force due to gravity F_g and an upward drag force F_D due to air resistance:

$$F_g = m \cdot g$$

Where m is the mass of UAV and g is the gravitational acceleration (9.81 m/s2).

$$F_D = \frac{1}{2} \cdot C_D \cdot A_C \cdot \rho_A \cdot V_T{}^2$$

Where C_D is the drag coefficient that depends on UAV shape and surface roughness and this study adopts $C_D = 0.3$, the same value as The UAS Task Force adopts (*Task Force Recommendations Final Report*, November 21,2015), ρ_A is the density of air (1.225kg/m3 at sea level), V_T is the true airspeed that is assumed to be the actual UAV velocity and A_C is the cross-sectional area of UAV:

$$A_C = \pi \cdot r_{UAV}{}^2$$

Where r_{UAV} is the characteristic radius that is used to define the UAV geometry as a circle. Recall that this study assumes that the failed UAV is at rest at the start of falling, the initial velocity is zero and the acceleration of the UAV gives:

$$a = \frac{F_g - F_D}{m}$$

The final velocity of the failed UAV (the collision velocity) could be expressed as:

$$V = \int_0^t a\,dt$$

Then we have:

$$V = \sqrt[2]{\frac{2mg}{C_D A_C \rho_A}(1 - e^{-\frac{hC_D A_C \rho_A}{m}})}$$

Where h equals to:

$$h = h_{UAV} - h_{human}$$

The height of a human h_{human} is assumed to be 1.7m and h is range between 0 and 120m since the maximum allowable height of the unmanned aircraft above ground level by regulation is $h_{UAV} = 400ft \approx 122m.$

The impact kinetic energy gives:

$$E = \frac{1}{2} \cdot m \cdot V^2$$

With the model UAV data and the formulas above, the theoretical impact kinetic energy can be simulated as below plot:

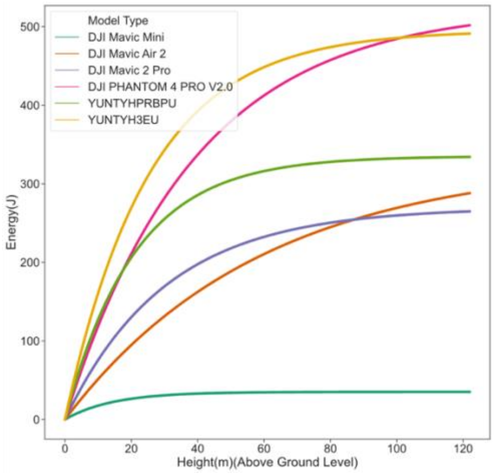

Kinetic Energy(J) Weight	Height (Above Ground Level)												
	5 m	10 m	15 m	20 m	25 m	30 m	40 m	45 m	50 m	55 m	60 m	100 m	122 m
0.249 kg	10.3	17.6	22.7	26.4	28.9	30.8	32.9	33.6	34.0	34.3	34.6	35.0	35.1
0.570 kg	26.8	51.4	74.1	94.8	113.9	131.5	162.4	176.0	188.5	200.0	210.5	269.2	288.1
0.907 kg	41.0	75.8	105.3	130.3	151.5	169.4	197.6	208.6	217.9	225.7	232.4	259.7	264.8
1.375 kg	63.3	118.9	167.9	210.9	248.8	282.0	337.2	359.6	379.5	397.0	412.4	484.5	501.8
1.633 kg	71.2	127.3	171.5	206.3	233.7	255.3	285.6	296.1	304.5	311.0	316.1	332.4	334.2
1.985 kg	88.4	161.0	220.7	269.7	309.9	343.0	392.5	410.8	425.9	438.3	448.5	485.6	491.2

4.2 IMPACT OF KINETIC ENERGY: ABBREVIATED INJURY SCORE

The Abbreviated Injury Score (AIS) is worldwide using standard classification in assessing injury and its injury severity level coded as integers from 0 for uninjured to 6 for fatal. The relationship between AIS and impact force (F) is shown as below table: (Dr. A.R. Payne)

Injury Level (AIS)	Tolerance Level (KN)
1 No Skull Fracture	$0 \leq F < 2.2$
2 Minor Depressed Skull Fracture	$2.2 < F \leq 5.5$
3 Major Depressed Skull Fracture	$5.5 < F \leq 11$
4 Severe Life-Endangering Fracture	$F > 11$

Based on the test result done by David Raymond (Raymond, Van Ee, Crawford, & Bir, 2009), below table shows the relationship between the kinetic energy and the impact force:

Velocity (m/s)	Kinetic Energy (J)	Impact Force (N)
22.2	24.6	3022
23.4	27.4	6347
19.6	19.8	3665
17.3	15.4	3171
16.3	13.7	2480
18.0	16.7	3551
19.5	19.6	3376
32.1	51.5	5724
34.2	58.5	9529
35.1	63.4	4701
31.9	52.4	5975
34.4	60.9	4977
35.2	63.8	6207
32.4	54.1	3547

We now estimate the energy threshold for each injury level with different regression models:

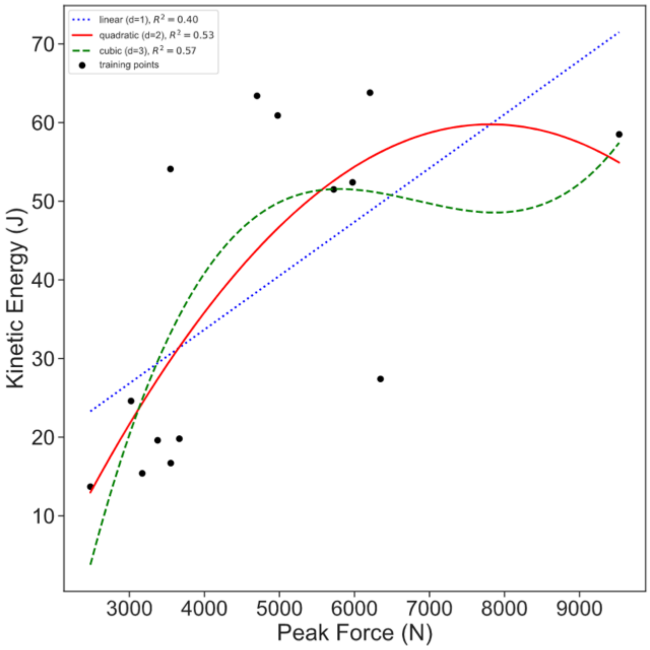

Compared with quadratic and cubic regression, this study adopts linear regression for kinetic energy estimation:

$$E = 0.00684073F + 6.31791824$$

Where F is the impact force.

Injury Level (AIS)	Tolerance Level (KN)	Kinetic Energy (J)
0-1 No Skull Fracture	$0 \leq F < 2.2$	$0 \leq E < 21.36$
2 Minor Depressed Skull Fracture	$2.2 < F \leq 5.5$	$21.36 < E \leq 43.94$
3 Major Depressed Skull Fracture	$5.5 < F \leq 11$	$43.94 < E \leq 81.57$
4 Severe Life-Endangering Fracture	$F > 11$	$E > 81.57$

With the obtained relationship between Impact Force and Injury Level, the simulated maximum allowable height for different UAV weights under different injury levels is given by below table:

AIS	Height (Above Ground Level)										
Weight	1 m	3 m	5 m	7 m	9 m	11 m	13 m	15 m	17 m	19 m	122 m
0.249 kg	AIS 1	AIS 1	AIS 1	AIS 1	AIS 1	AIS 1	AIS 1	AIS 2	AIS 2	AIS 2	AIS 2
0.570 kg	AIS 1	AIS 1	AIS 2	AIS 2	AIS 3	AIS 3	AIS 3	AIS 3	AIS 4	AIS 4	AIS 4
0.907 kg	AIS 1	AIS 2	AIS 2	AIS 3	AIS 3	AIS 4	AIS 4	AIS 4	AIS 4	AIS 4	AIS 4
1.375 kg	AIS 1	AIS 2	AIS 3	AIS 4	AIS 4	AIS 4	AIS 4	AIS 4	AIS 4	AIS 4	AIS 4
1.633 kg	AIS 1	AIS 3	AIS 3	AIS 4	AIS 4	AIS 4	AIS 4	AIS 4	AIS 4	AIS 4	AIS 4
1.985 kg	AIS 1	AIS 3	AIS 4	AIS 4	AIS 4	AIS 4	AIS 4	AIS 4	AIS 4	AIS 4	AIS 4

4.3 PROBABILITY OF IMPACT

David Raymond conducted the experimental research for prediction of skull fracture due to blunt ballistic temporo-parietal head impact (Raymond et al., 2009) and a logistic regression model developed from his research to determine the relationship between force and probability of fracture is given by:

$$P_{Skull\ Fracture} = \frac{1}{1 + e^{-(-3.592+0.001F)}}$$

The fit curve represents above model is shown as below figure:

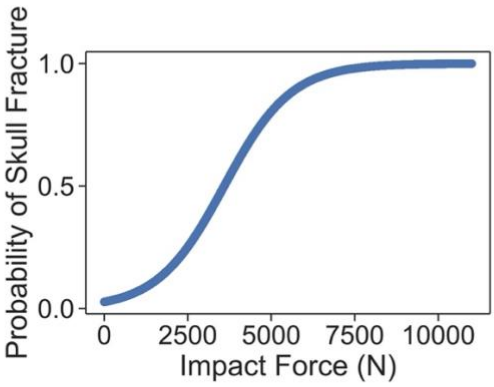

With the given logistic regression model of fracture probability, we can now estimate the probability of skull fracture for each Injury Level:

Injury Level (AIS)	Tolerance Level (KN)	Skull Fracture Probability
0-1 No Skull Fracture	$0 \le F < 2.2$	$0.027 \le P < 0.199$
2 Minor Depressed Skull Fracture	$2.2 < F \le 5.5$	$0.199 < P \le 0.870$
3 Major Depressed Skull Fracture	$5.5 < F \le 11$	$0.870 < P \le 0.999$
4 Severe Life-Endangering Fracture	$F > 11$	$P > 0.999$

With the equation of probability of skull fracture, the probability of skull fracture under certain kinetic energy can be calculated.

4.4 PROBABILITY OF CERTAIN NUMBER OF PEOPLE BEING EXPOSED TO MISHAP

Acquiring quality population density data is often the bottleneck in estimating casualty risk due to its dynamic nature. A more accurate representation of population density and movement is paramount for studies in natural disasters and accidents/incidents.

In order to better capture and demonstrate number of people N_C within certain environment (each administrative urban region in Singapore), this study explores the dataset of Singapore population density(2020), Singapore region boundary, the entire Cadastral Airspace map of Singapore acquired from (Network (CIESIN), Columbia University (2018)), (SLA, 2020), (SLA, 2010) respectively for visualizing the dataset using QGIS (QGIS.org, 2020) as given in below figure. The population density data provides estimated total number of people per grid-cell within the area of interest at a resolution of 3 arc (approximately 100m at the equator).

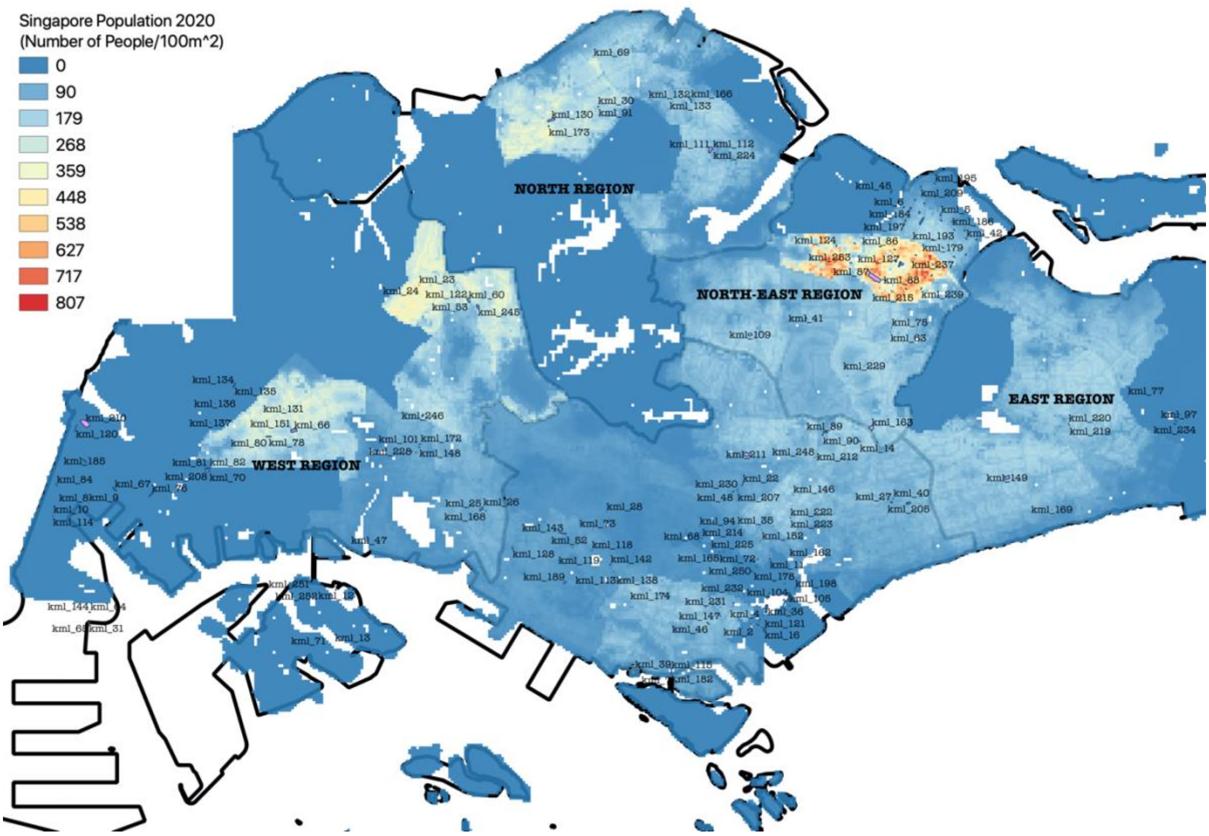

In a free fall vertical crash, the casualty area A_C gives:

$$A_C = \pi \cdot (r_{UAV} + r_{human})^2$$

According to Weidmann (Ulrich Weidmann; Transporttechnik der Fuàgänger; Institut fâr Verkehrsplanung, Transporttechnik, Straàen- und Eisenbahnbau Zârich; Schriftreihe des IVT Nr. 90; 2. Ergänzte Auflage; März 1993.), the average citizen of Central Europe has a minimum space requirement of 0.085 m2, then we have:

$$A_C = \ 0.085 + \pi \cdot {r_{UAV}}^2$$

Assume that people can be randomly located anywhere inside a populated area A_P, the probability that certain number of people x being exposed to a UAV mishap follows a binominal distribution and can be expressed as:

$$P(X) = \frac{N_C!}{(N_C - X)!\,X!}\ (\frac{A_C}{A_P})^X(1 - \frac{A_C}{A_P})^{N_C - 1}$$

Where $\frac{A_C}{A_P}$ is the probability of a specific person being exposed to a UAV mishap.

The final probability of casualty is given by:

$$P(C) = P(X)P_{Skull\ Fracture}$$

5. RISK CONSTRUCT

For the purposes of risk evaluation and demonstration, this study adopts the modified (Ancel, Capristan, Foster, & Condotta) Specific Operation Risk Assessment (SORA) methodology developed by Joint Authorities for Rulemaking on Unmanned Systems (JARUS) for evaluating the UAV risk related to a given operation. The reference of the acceptable thresholds for severity (minimal, minor, major, catastrophic) and likelihood (frequent, probable, remote, and improbable) is given as below table.

Severity / Likelihood	Minimal $0 \leq P_{casualty} < 0.25$	Minor $0.25 \leq P_{casualty} < 0.5$	Major $0.5 \leq P_{casualty} < 0.75$	Catastrophic $0.75 \leq P_{casualty} \leq 1$
Frequent $0.2 \leq P_{mishap} < 1$	Low	Medium	High	High
Probable $0.1 \leq P_{mishap} < 0.2$	Low	Medium	High	High
Remote $0.01 \leq P_{mishap} < 0.1$	Low	Medium	Medium	High
Improbable $0 \leq P_{mishap} < 0.01$	Low	Low	Medium	High

6. REFERENCE

Abdallah, R. (2019). *Reliability approaches in networked systems : Application on Unmanned Aerial Vehicles.*

Ancel, E., Capristan, F. M., Foster, J. V., & Condotta, R. C. In-Time Non-Participant Casualty Risk Assessment to Support Onboard Decision Making for Autonomous Unmanned Aircraft. In *AIAA Aviation 2019 Forum*.

Ancel, E., Capristan, F. M., Foster, J. V., & Condotta, R. C. (2019). *In-Time Non-Participant Casualty Risk Assessment to Support Onboard Decision Making for Autonomous Unmanned Aircraft*.

Ancel, E., Shih, A., Jones, S., Reveley, M., Luxhøj, J., & Evans, J. (2015). Predictive safety analytics: Inferring aviation accident shaping factors and causation. *Journal of Risk Research, 18*. doi:10.1080/13669877.2014.896402

CAAS. (2019). *UA Operator and Activity Permits*. Retrieved from https://www.caas.gov.sg/public-passengers/unmanned-aircraft/ua-regulatory-requirements/ua-operator-and-activity-permits

Dr. A.R. Payne, S. P. Injury Mechanisms & Injury Criteria. Retrieved from http://www.eurailsafe.net/subsites/operas/HTML/Section3/Section3.3frm.htm

Dzindolet, M. T., Pierce, L. G., Beck, H. P., Dawe, L. A., & Anderson, B. W. (2001). Predicting Misuse and Disuse of Combat Identification Systems. *Military Psychology, 13*(3), 147-164. doi:10.1207/S15327876MP1303_2

Hart, S. G., & Staveland, L. E. (1988). Development of NASA-TLX (Task Load Index): Results of Empirical and Theoretical Research. In P. A. Hancock & N. Meshkati (Eds.), *Advances in Psychology* (Vol. 52, pp. 139-183): North-Holland.

Heckerman, D. (2008). A Tutorial on Learning With Bayesian Networks. In (Vol. 156, pp. 33-82).

Jensen, F., & Nielsen, T. (2001). *Bayesian Networks and Decision Graphs*.

Kok, L. M. (2015). CAAS launches online portal for drone permit applications in Singapore. *The Straits Times Singapore*. Retrieved from http://www.straitstimes.com/singapore/caas-launches-online-portal-for-drone-permit-applications-in-singapore.

Network (CIESIN), Columbia University (2018), S. o. G. a. E. S. U. o. S. D. o. G. a. G. U. o. L. D. d. G. U. d. N. a. C. f. I. E. S. I.

Nguyen, T., Lim, C. P., Nguyen, N. D., Gordon-Brown, L., & Nahavandi, S. (2019). A Review of Situation Awareness Assessment Approaches in Aviation Environments. *IEEE Systems Journal, 13*(3), 3590-3603. doi:10.1109/JSYST.2019.2918283

QGIS.org. (2020). QGIS Geographic Information System. In.

Raymond, D., Van Ee, C., Crawford, G., & Bir, C. (2009). Tolerance of the skull to blunt ballistic temporo-parietal impact. *Journal of Biomechanics, 42*(15), 2479-2485. doi:https://doi.org/10.1016/j.jbiomech.2009.07.018

Reid, G. B., & Nygren, T. E. (1988). The Subjective Workload Assessment Technique: A Scaling Procedure for Measuring Mental Workload. In P. A. Hancock & N. Meshkati (Eds.), *Advances in Psychology* (Vol. 52, pp. 185-218): North-Holland.

SLA. (2010). *SLA Cadastral Land Parcel*. Retrieved from: https://data.gov.sg/dataset/sla-cadastral-land-parcel?resource_id=60f3d2ca-e058-4a7a-9dbc-5b7df2d9cd19

SLA. (2020). *SLA Cadastral Airspace Parcel*. Retrieved from: https://data.gov.sg/dataset/sla-cadastral-airspace-parcel?resource_id=592c929d-219d-4943-976d-cefb8a0c1d06

Task Force Recommendations Final Report. (November 21,2015). Retrieved from https://www.faa.gov/regulations_policies/rulemaking/committees/documents/media/UASRTFARC-102015.pdf